Free-Form Deformation Using Lower-Order B-spline for Nonrigid Image Registration

Wei Sun[1], Wiro J. Niessen[1,2], and Stefan Klein[1]

[1] Biomedical Imaging Group Rotterdam, Erasmus MC, Rotterdam, The Netherlands
{w.sun,w.niessen,s.klein}@erasmusmc.nl
[2] Department of Image Science and Technology, Faculty of Applied Sciences, Delft University of Technology, Delft, The Netherlands

Abstract. In traditional free-form deformation (FFD) based registration, a B-spline basis function is commonly utilized to build the transformation model. As the B-spline order increases, the corresponding B-spline function becomes smoother. However, the higher-order B-spline has a larger support region, which means higher computational cost. For a given D-dimensional nth-order B-spline, an mth-order B-spline where $(m \leq n)$ has $(\frac{m+1}{n+1})^D$ times lower computational complexity. Generally, the third-order B-spline is regarded as keeping a good balance between smoothness and computation time. A lower-order function is seldom used to construct the deformation field for registration since it is less smooth. In this research, we investigated whether lower-order B-spline functions can be utilized for efficient registration, by using a novel stochastic perturbation technique in combination with a postponed smoothing technique to higher B-spline order. Experiments were performed with 3D lung and brain scans, demonstrating that the lower-order B-spline FFD in combination with the proposed perturbation and postponed smoothing techniques even results in better accuracy and smoothness than the traditional third-order B-spline registration, while substantially reducing computational costs.

1 Introduction

The B-spline based FFD registration is a popular approach for nonrigid registration. In general, the third-order B-spline is utilized to model the transformation in B-spline FFD method. B-spline functions with different orders are a series of convolutional basis functions. The nth-order B-spline function is n times convolution of the zeroth-order B-spline. As the n goes to infinity, B-splines converge to a Gaussian function with an infinite support. The smoothness is improved as the growth of B-spline order. However, this improvement is accompanied by the increasing computational cost because of a larger support which means more control points have to be involved in computation.

Our previous work [1] has initially investigated by using the randomly shifted second-order B-spline with uniform distribution to simulate third-order B-spline method. In this work, we extend the whole theoretical framework into a statistical view, go down to the first and zeroth orders of B-splines, and introduce

P. Golland et al. (Eds.): MICCAI 2014, Part I, LNCS 8673, pp. 194–201, 2014.

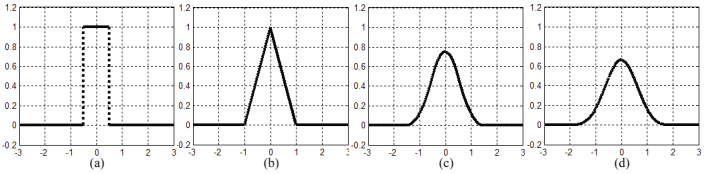

Fig. 1. One-dimensional B-splines with four different orders: (a) $\beta^0(x)$; (b) $\beta^1(x)$; (c) $\beta^2(x)$; (d) $\beta^3(x)$

the Gaussian perturbation to the framework. The performances of lower-order B-splines for nonrigid registration were evaluated in terms of registration accuracy, smoothness and efficiency.

2 Method

2.1 B-spline Basis Functions

In B-spline FFD registration method, B-spline functions are equally placed on a D-dimensional uniform control-point grid. The nth-order B-spline function is obtained by n times convolution of the zeroth-order B-spline functions,

$$\beta^n(x) = \beta^0(x) \underbrace{* \cdots * \beta^0(x)}_{n \text{ times}}, \tag{1}$$

where $\beta^0(x)$ is fixed to be 1 when $(-0.5 \leq x < 0.5)$ and the operator '$*$' denotes the convolution operation. Figure 1 presents the curves of $\beta^0(x)$, $\beta^1(x)$, $\beta^2(x)$, and $\beta^3(x)$. With increasing spline order, the smoothness improves, but the support (nonzero domain) becomes larger. For a D-dimensional transformation model, the tensor product of $\beta^n(x)$ is used to span a multidimensional B-spline basis function $\Phi_D^n(\mathbf{x})$.

2.2 Registration Framework

B-splines based FFD registration is a parametric intensity-based type of registration method. The D-dimensional fixed and moving images are denoted as $F(\mathbf{x}) : \Omega_F \subset \mathcal{R}^D \rightarrow \mathcal{R}$ and $M(\mathbf{x}) : \Omega_M \subset \mathcal{R}^D \rightarrow \mathcal{R}$ where $\mathbf{x} \in \mathcal{R}^D$ represents an image coordinate. Then, the registration problem is defined as:

$$\hat{\boldsymbol{\mu}} = \arg\min_{\boldsymbol{\mu}} \mathcal{C}(F, M(\mathbf{T}_{\boldsymbol{\mu}}(\mathbf{x}))), \tag{2}$$

where $\mathcal{C}$ represents the dissimilarity measurement between the fixed image and the transformed moving image, $\mathbf{T}_{\boldsymbol{\mu}}(\mathbf{x}) : \Omega_F \rightarrow \Omega_M$ is a coordinate transformation, and $\boldsymbol{\mu}$ represents the parameter vector of the transformation model.

A comparison of different optimizers [2] has shown that the stochastic gradient descent (SGD) method is a competitive alternative to deterministic methods. In SGD, the "optimization direction" is a stochastic approximation of $\partial\mathcal{C}/\partial\boldsymbol{\mu}$,

$$\boldsymbol{\mu}_{k+1} = \boldsymbol{\mu}_k - a_k\tilde{\boldsymbol{g}}(\boldsymbol{\mu}_k), \quad k = 1, 2, \ldots, K \tag{3}$$

where $\tilde{\boldsymbol{g}}(\boldsymbol{\mu}_k)$ represents the approximate derivative of the cost function evaluated at the current optimization position $\boldsymbol{\mu}_k$. In [2] the stochastic approximation was calculated by evaluating the cost function derivative on a small random subset $\widetilde{\Omega}_F \subset \Omega_F$ of image samples, newly selected in each iteration k, thus reducing the computation time per iteration. To guarantee the convergence of stochastic optimization, step size a_k is defined as a decaying function of k in most theoretical work. In [3] an adaptive strategy for automatically setting a_k was proposed. This adaptive SGD (ASGD) optimizer is used in this work.

2.3 B-spline FFD

The traditional FFD transformation model [4] is defined as

$$\mathbf{T}^n_{\boldsymbol{\mu}}(\mathbf{x}) = \mathbf{x} + \sum_{\boldsymbol{\xi}\in\Xi} \mathbf{c}_{\boldsymbol{\xi}} \Phi^n_D(\mathbf{x}/\eta - \boldsymbol{\xi}), \tag{4}$$

where $\Xi \subset \mathcal{Z}^D$ denotes a D-dimensional uniform control-point grid, η is the grid spacing, $\mathbf{c}_{\boldsymbol{\xi}}$ represents the coefficient vector for a control point $\boldsymbol{\xi}$, and the vector of transformation parameters $\boldsymbol{\mu}$ is constructed from the elements of all coefficient vectors ($\boldsymbol{\mu} = \{\mathbf{c}_{\boldsymbol{\xi}} \mid \boldsymbol{\xi} \in \Xi\}$). As described in Section 2.2, a stochastic approximation of the derivative $\partial\mathcal{C}/\partial\boldsymbol{\mu}$ is calculated in the SGD based registration, which requires evaluation of transformation and its derivative.

Therefore, the size of the support of B-spline function has a significant influence to the computational cost of registration.

2.4 Random Perturbation and Postponed Smoothing

Random perturbation and postponed smoothing techniques are derived from the convolutional property of B-spline function. If the nth-order B-spline function is utilized to model the transformation, the number of control points considered in each dimension is $n+1$ inside the support region. Then, the number of control points for a D-dimensional transformation is $(n+1)^D$. In practical medical image registration tasks, the input images F and M are usually 3D images. Thus, the numbers of control points which need to be considered around one image coordinate are 64, 27, 8, and 1 for $\beta^3(x)$, $\beta^2(x)$, $\beta^1(x)$, and $\beta^0(x)$, respectively. As introduced in Section 2.3, the computational cost of nonrigid registration is dominated by evaluating the transformation and its derivative. Therefore, the computational cost could be significantly reduced if lower-order B-spline function could replace the commonly used third-order B-splines.

From Eq.(1) and the convolution operation, we derive

$$\beta^n(x) = (\beta^m * \beta^{n-m-1})(x) = \int_{-\infty}^{\infty} \beta^m(x-t)\beta^{n-m-1}(t)dt = \int_{-\infty}^{\infty} \beta^m(x-t)p(t)dt, \tag{5}$$

where $m \leq n$ and $p(t)$ represents the probability density function (PDF) corresponding to $\beta^{n-m-1}(t)$. For example, $p(t)$ is a uniform PDF as the box function $\beta^0(t)$ when $m = n-1$, or $p(t)$ is a Dirac delta PDF for the conventional non-perturbed FFD registration. Therefore, $\beta^n(x)$ can be considered as a mathematical expectation of $\beta^m(x-t)$ with the given PDF $p(t)$, and $\beta^m(x-t)$ is a shifted $\beta^m(x)$. Inspired by this relation, we propose to construct an expected B-spline FFD by randomly shifting lower-order B-splines $\beta^m(x-t)$ with $p(t)$.

This leads to the following definition of random perturbation transformation model

$$\widetilde{\mathbf{T}}^m_{\boldsymbol{\mu}}(\mathbf{x}, \mathbf{t}) = \mathbf{x} + \sum_{\boldsymbol{\xi} \in \Xi} \mathbf{c}_{\boldsymbol{\xi}} \Phi^m_D(\mathbf{x}/\eta - \boldsymbol{\xi} - \mathbf{t}), \tag{6}$$

where m is the order of lower-order B-spline, $\mathbf{t} = [t_1, t_2, \cdots, t_D]^T$ denote the random shifts in each dimension. Through this way, the entire B-spline control point grid is thus shifted by vector $\mathbf{t}$ but the grid layout is kept.

As introduced in Section 2.1, a higher-order B-spline is convolved from lower-order B-splines. Therefore, to smooth the transformation field recovered by a lower-order B-spline function with a higher-order B-spline, the postponed smoothing technique is further proposed.

The new random perturbation and postponed smoothing techniques fit naturally in the framework of stochastic gradient descent optimization. For the computation of $\partial \mathcal{C}/\partial \boldsymbol{\mu}$, we use $\widetilde{\mathbf{T}}^m_{\boldsymbol{\mu}}(\mathbf{x}, \mathbf{t})$ instead of $\mathbf{T}^n_{\boldsymbol{\mu}}(\mathbf{x})$, with a perturbation $\mathbf{t}$ randomly chosen in each iteration k of optimization. We thus obtain a stochastic approximation of the true derivative, at a lower computational cost. It is worth to note that this approximation comes on top of the approximation by randomly subsampling the image as explained in Section 2.2. The optimization procedure therefore can be described as

$$\boldsymbol{\mu}_{k+1} = \boldsymbol{\mu}_k - a_k \tilde{\boldsymbol{g}}(\boldsymbol{\mu}_k, \mathbf{t}_k), \tag{7}$$

where $\mathbf{t}_k$ is the realization of $\mathbf{t}$ in iteration k. The computationally efficient mth-order B-spline function is utilized only during the optimization process. The postponed smoothing approach is applied to the lower-order transformation field once the stochastic gradient descent optimization has finished. Through this way, the estimated parameters $\hat{\boldsymbol{\mu}}$ are directly plugged into a higher-order B-spline FFD to obtain the final transformation. Please note that the random perturbation and postponed smoothing techniques can be used separately or combined together in a sequential way for later comparison.

In the present work, we focused on B-splines with the highest order $n = 3$. The standard third-order B-spline registration method is defined as the reference method. For a clear comparison, the whole registration process with lower-order B-spline is divided into three components (Perturbation-Optimization-Postponed

smoothing) which are denoted as $(< p(t) > - < m > - < n >)$ where $p(t) \in \{\text{Uniform, Gaussian, Dirac delta}\}$, $m \in \{0, 1, 2\}$ and $n \in \{0, 1, 2, 3\}$. If the perturbation process is used, $p(t)$ can be assigned with uniform PDF $(\beta^0(t))$ or its corresponding truncated Gaussian PDF. The options of these components should be combined together to create a candidate registration method under the restriction that only higher or equal order $(n \geq m)$ is allowed for postponed smoothing. Besides the conventional third-order B-spline, we compared 27 possible combinations in the experiments. In the following parts, the naming rule $(< p(t) > - < m > - < n >)$ is used for shorthand notation for each registration method. For example, Dirac-3-3 denotes the conventional third-order B-spline registration method. Algorithm 1 provides an overview of the proposed registration method.

Input: $F \leftarrow$ fixed image, $M \leftarrow$ moving image, $K \leftarrow$ number of iterations,
$S \leftarrow$ number of samples $|\widetilde{\Omega}_F|$, $m \leftarrow$ B-spline order for optimization,
$n \leftarrow$ B-spline order for final transformation, and
$p(\mathbf{t}) \leftarrow$ Uniform, Gaussian or Dirac delta

Output: Registered moving image $M\left(\mathbf{T}^n_{\hat{\boldsymbol{\mu}}}(\mathbf{x})\right)$

Initialize transformation parameters $\boldsymbol{\mu} \leftarrow \mathbf{0}$
for $k \leftarrow 1$ *to* K **do**
  Initialize random samples $[\mathbf{x}_1 \ldots \mathbf{x}_S]$, $\tilde{\boldsymbol{g}} = \mathbf{0}$ and step size a_k
  Draw random perturbation $\mathbf{t}_k \leftarrow p(\mathbf{t})$
  for $\mathbf{x} \leftarrow \mathbf{x}_1$ *to* $\mathbf{x}_S$ **do**
    Evaluate $F(\mathbf{x})$, and $\mathbf{y} \leftarrow \widetilde{\mathbf{T}}^m_{\boldsymbol{\mu}}(\mathbf{x}, \mathbf{t}_k)$
    Interpolate moving image value $M(\mathbf{y})$, and calculate gradient $\nabla M(\mathbf{y})$
    $\partial \widetilde{\mathbf{T}}^m_{\boldsymbol{\mu}}(\mathbf{x}, \mathbf{t}_k)/\partial \boldsymbol{\mu}$, and calculate contribution to $\tilde{\boldsymbol{g}}$
  end
  Update transformation parameters $\boldsymbol{\mu} \leftarrow \boldsymbol{\mu} - a_k \tilde{\boldsymbol{g}}$
end
$\hat{\boldsymbol{\mu}} \leftarrow \boldsymbol{\mu}$
Instantiate nth-order FFD transformation $\mathbf{T}^n_{\hat{\boldsymbol{\mu}}}(\mathbf{x})$,and **return** $M\left(\mathbf{T}^n_{\hat{\boldsymbol{\mu}}}(\mathbf{x})\right)$

Algorithm 1. Proposed registration method

3 Experiments

The open source image registration package `elastix` [5] was used to implement all registration methods. For lung and brain data, similarity measures sum of squared differences (SSD), normalized correlation coefficient (NCC) were used as dissimilarity terms, respectively. For the ASGD optimizer, the numbers of random samples S and iterations K were set to 2000 in all experiments. To create 4 image resolution levels of input images, a Gaussian filter using $\{\sigma_1, \ldots, \sigma_4\} = \{4, 2, 1, 0.5\}$ voxels was applied. During the registration, the transformation of a finer scale was initialized by the transformation estimated at the coarser scale. The grid schedules $\{\eta_1, \eta_2, \eta_3, \eta_4\}$=$\{64, 32, 16, 8\}$mm and $\{64, 38, 22, 13\}$mm were used on lung data. On the brain data, the grid schedule $\{40, 20, 10, 5\}$mm was utilized. For the perturbation process, the standard deviation σ_{U} of uniform PDF changes with grid spacing η_i, but for the σ_{G} of Gaussian PDF we restricted it to be the σ_U on the finest grid spacing η_4.

Since the Gaussian PDF is not compactly supported, we truncated the Gaussian PDF using $min(\eta_i, 4 \times \sigma_{\mathrm{G}})$.

We used 10 pairs of DIR-Lab 3D chest CT scans with 300 manually annotated landmarks on the lung structure. The voxel and dimension sizes of lung data are around $1 \times 1 \times 2.5$mm and around $256 \times 256 \times 110$. Lung masks were created to constraint the registration on the lung region. For all cases, the exhale phase (moving image) was registered to the inhale phases (fixed image). The mean target registration error (mTRE) which calculates the distance between the transformed and ground truth landmarks was used to measure the registration accuracy. To evaluate the transformation smoothness of registration, the standard deviation of the determinant of spatial Jacobian D_{SJ} was calculated inside lung mask. The standard deviation of D_{SJ} represents the fluctuation of the estimated transformation field, and therefore gives an indication of the smoothness of a transformation.

The Internet Brain Segmentation Repository (IBSR v2.0), which contains 18 T1-weighted MRI 3D brain scans, was also used to evaluate the registration methods with inter-subject registration. The volumes of these images are $256 \times 256 \times 128$. The voxel sizes are around $1 \times 1 \times 1.5$mm. To evaluate the registration accuracy, overall mean overlap which measures the overlap between the transformed and ground truth atlases over all labels was used. To measure the smoothness of the transformation, we used the same standard deviation of D_{SJ} which was calculated inside a brain mask. The same affine registrations were used to roughly align the data first for each registration method.

4 Results

Figure 2 (a) plots a 2D average rank in terms of accuracy and smoothness based on the results from the 20 test cases for each methods on lung data. The X-axis and Y-axis indicate the ranking in registration accuracy and smoothness ,and the lower ranking number means better performance. From Figure 2 (a), both $m = 2$ and $m = 1$ methods can produce better accuracy and smoothness than the traditional third-order B-spline method with proper perturbation and postponed smoothing techniques. The green line in Figure 2 (a) shows the trace of improved rank by uniform perturbation and followed by the third-order postponed smoothing. Similarly, the blue line indicates the trace of improved ranks in both accuracy and smoothness by only the postponed smoothing technique.

On the lung data, the results of several typical methods using the finest grid spacings 13mm and 8mm were pooled and shown as box plots in Figure 3 (a) and (b). Overall, the lower-order B-spline registration can generate better accuracy and smoothness than the conventional third-order registration method (Dirac-3-3). Since the calculation of spatial Jacobian on Dirac-0-0 is impossible, its blank position is marked as black cross in Figure 3 (b).

The 2D ranks of 28 registration methods on the brain data are shown in Figure 2 (b). Compared with the rank of third-order B-spline, the lower-order B-spline can also generate better accuracy and smoothness on brain data. Because the overlap measurement is less sensitive to the smoothness, the first-order

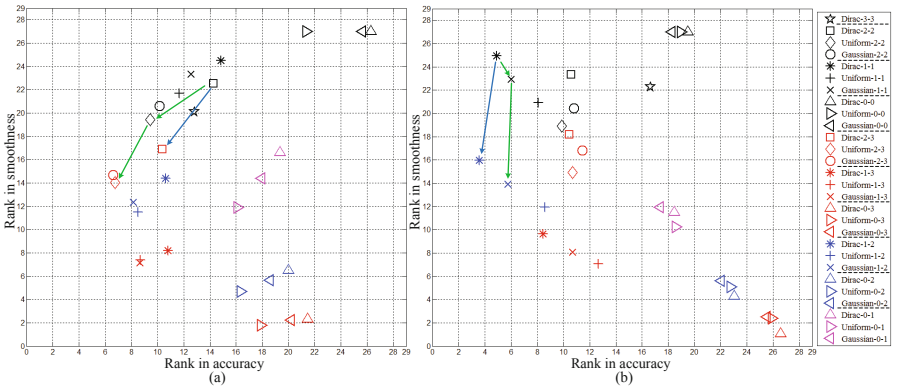

Fig. 2. Two dimensional averaged ranking number of different methods: (a) lung data; (b) brain data

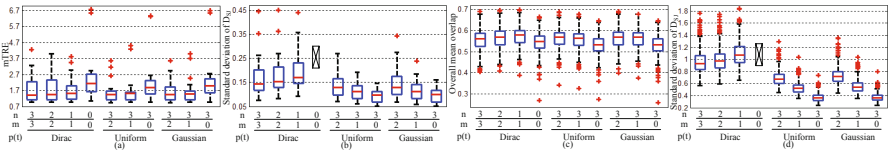

Fig. 3. Registration results by different methods: (a) accuracy on lung data (mTRE, in mm, lower values are better); (b) smoothness on lung data (standard deviation of D_{SJ}, lower values are better); (c) accuracy on brain data (overall mean overlap, higher values are better); (d) smoothness on brain data (standard deviation of D_{SJ}, lower values are better)

B-spline is more favorable on brain data than the second-order B-spline on lung data. The green and blue lines indicate the trace of rank change after the random perturbation and postponed smoothing technique. By applying these two techniques, more adjacent image information is considered during registration. Therefore, the smoothness is improved more significantly than accuracy. The detailed registration results of several typical methods are provided in Figure 3 (c) and (d).

Experimentally, the computation time on lung (subject No.3) using an Intel Core i7-2720QM with 8G memory were 149.4 ± 1.7 seconds, 90.1 ± 1.1 seconds, 64.9 ± 0.9 seconds, and 53.5 ± 0.5 seconds (mean $\pm$ standard deviation over 10 runs) for the methods with B-spline orders third, second, first, and zeroth during optimization, respectively. On the brain data (registering subject No.6 to subject No.8) were 223.7 ± 1.3 seconds, 145.0 ± 0.7 seconds, 115.5 ± 1.6 seconds, and 103.7 ± 0.7 seconds for B-spline orders from third to zeroth, respectively.

5 Discussion

The improvements on accuracy and smoothness show that both random perturbation process and postponed smoothing technique are essential for good registration performance. According to the accuracy and smoothness on lung and brain data, Gaussian-1-3, Uniform-1-3 and Dirac-1-3 produced consistently better registration results. There are two possible explanations for the improved registration results. First, in perturbation process, a new stochastic dynamic is introduced to the stochastic gradient descent optimization. The stochastic perturbations may help to avoid the local minima as has been previously reported in the literature on stochastic approximation optimization [6]. Second, due to the disproportionate B-spline weighting of the control points [7], the traditional B-spline FFD can lead to ill-conditioned optimization spaces. In current work, the influences of different control points to the cost function are randomly changed in each iteration by randomly shifting the control point grid. Thus, the disadvantage of the disproportionate control point weighting might be alleviated by the perturbation process. The current stochastic perturbation process was derived from the convolutional property of B-spline functions. In the future, we could also test the potential of the perturbation process on other basis functions.

6 Conclusions

In this work, the potential of FFD registration based on lower-order B-spline was investigated. With the proposed random perturbation and postponed smoothing approaches, the lower-order B-spline FFD method produced better registration accuracy and smoothness than the popular third-order B-spline registration method. Because less control points are involved in the lower-order B-spline registration, the method is computationally less expensive than the traditional approach.

References

1. Sun, W., Niessen, W.J., Klein, S.: Randomly perturbed free-form deformation for nonrigid image registration. In: Ourselin, S., Modat, M. (eds.) WBIR 2014. LNCS, vol. 8545, pp. 62–71. Springer, Heidelberg (2014)
2. Klein, S., et al.: Evaluation of optimization methods for nonrigid medical image registration using mutual information and B-splines. IEEE Trans. Image Process. 16(12), 2879–2890 (2007)
3. Klein, S., et al.: Adaptive stochastic gradient descent optimisation for image registration. Int. J. Comput. Vis. 81(3), 227–239 (2009)
4. Rueckert, D., et al.: Nonrigid registration using free-form deformations: Application to breast MR images. IEEE Trans. Med. Imag. 18(8), 712–721 (1999)
5. Klein, S., et al.: Elastix: a toolbox for intensity-based medical image registration. IEEE Trans. Med. Imag. 29(1), 196–205 (2010)
6. Maryak, J., et al.: Global random optimization by simultaneous perturbation stochastic approximation. IEEE Trans. Automat. Contr. 53(3), 780–783 (2008)
7. Tustison, N.J., et al.: Directly manipulated free-form deformation image registration. IEEE Trans. Image Process. 18(3), 624–635 (2009)